Available online at www.sciencedirect.com
SCIENCE DIRECT
Catalysis Today 101 (2005) 175–183
CATALYSIS TODAY
www.elsevier.com/locate/cattod

A comparison of the electronic structure and NO adsorption on the (0 0 1)-V_2O_5 surfaces and (0 0 1)-V_2O_5 surfaces with Mo defects—DFT cluster studies

P. Kornelak, A. Michalak *, M. Najbar

Faculty of Chemistry, Jagiellonian University, Ingardena 3, 30-060 Cracow, Poland

Available online 7 March 2005

Abstract

DFT calculations were performed for models of the (0 0 1) surfaces of non-reduced and reduced vanadia, represented by $V_{12}O_{30}$ and $V_{12}O_{29}$ clusters, as well as for models of (0 0 1) V_2O_5 surfaces with Mo defects, represented by $V_{11}MoO_{30}$ and $V_{11}MoO_{29}$ clusters. The clusters were embedded in a set of point charges in order to consider electrostatic bulk influence. Surface reduction was modeled by the removal of vanadyl/molybdenyl oxygen. Analysis of the electronic structure in all the clusters was conducted in terms of the Mulliken population analysis, Mayer bond-orders, atomic Fukui function values, and molecular electrostatic potential (MEP) distribution. The results show that substituting a V atom with Mo leads to a reduction of the adjacent metal atom, practically without changing the electronic properties of the oxygen atoms. Furthermore, the NO adsorption on the reduced surfaces of V_2O_5 and V_2O_5 with Mo defects has been studied. In all cases, adsorption is exothermic; the energetic stabilization is the largest for the $V_{11}MoO_{29}$ from which the molybdenyl atom was removed. However, the calculated adsorption energies are similar, within ca. 3 kcal/mol (12 kJ/mol). Thus, the effect of the molybdenum presence for energetic stabilization of adsorbed NO is not very distinct.

Keywords: Molybdena–vanadia solid solution; NO adsorption; DFT calculation; Molecular electrostatic potential; Fukui function

1. Introduction

Transition metal oxides still garner experimental and theoretical interest due to the great variety in their chemical and physical properties. Among the oxides, divanadium pentoxide and molybdenum trioxide are especially well known for their catalytic activity in numerous chemical processes. It has been found that divanadium pentoxide and molybdenum trioxide can form binary V–Mo–O oxide systems [1]. Vanadia supported on titania is known as a good catalyst for the selective reduction (SCR) of NO_x to N_2 by ammonia in the presence of oxygen. That process is commonly used for NO_x removal from off-gases of stationary sources of emission (e.g. power and heat plants, waste incineration, nitric acid production, and stationary diesel engines) [2–7]. Catalytic activity of titania-supported binary systems such as W–O–V/TiO_2 [8–10] or Mo–O–V/TiO_2 [11] in NO_x reduction is higher than titania-supported vanadia. Recently, there has been an increasing interest in the direct decomposition of NO. Catalytic activity of titania-supported binary systems W–O–V/TiO_2 and Mo–O–V/TiO_2 in that process has also been reported [12–16].

Vanadia, molybdena and titania-supported binary W–O–V/TiO_2 and Mo–O–V/TiO_2 systems were also investigated by theoretical methods. There exist numerous theoretical studies on the electronic structure and properties of vanadium and molybdenum oxides, from diatomic molecules VO [17–20] and MoO [17–22] as well as the corresponding ionic species [18,19,22,23], to oxide clusters in the gas phase [22,24,25], V_2O_5 and MoO_3 bulk [24,26–28], and the models of their surfaces [12,26,29–47]. In those studies both, semi-empirical [29,30,34–36,39,42,48], and ab initio (HF and DFT) [12,17–28,30–33,37–47,49–57] quantum-chemical approaches were used. Cluster models of the surfaces [12,27–52,54–57] as well as slab models

* Corresponding author. Tel.: +48 12 663 2217; fax: +48 12 634 0515.
E-mail address: michalak@chemia.uj.edu.pl (A. Michalak).

0920-5861/$ – see front matter © 2005 Elsevier B.V. All rights reserved.
doi:10.1016/j.cattod.2005.01.015

[24–26,37,42,53] were applied. The theoretical investigations focused on the properties of the oxide systems [12,24–28,30–47,50,52,54,57] as well as the reactions that occur on their surfaces, e.g. adsorption of H, H^+ [30,31,34,35,37–41,43,44,48,55] and desorption of hydroxyl groups [31,40,41,43,44] or water molecules [41,43,44], and the adsorption of hydrocarbons and their selective oxidation [29,30,34,39,40]. The influence of oxygen vacancies on the structure and properties of vanadia and molybdena have also been studied [27,36,38,41,43–45].

There are only a few reports of the theoretical studies on binary metal oxide systems. In [12,47,50–52,54], the studies on the V–O–W properties as well as the water adsorption [50,52,54] and dissociation [51,52,54] were reported. The effects of additives on the electronic and geometric structure of the active center of a vanadia-based catalyst for oxidative dehydrogenation of propane have been presented [57]. Interaction between V_2O_5 and TiO_2 have been investigated by Calatayud et al. [25] and Haber and Witko [46]. Similarly, only a little theoretical work has been done on the process of the SCR of NO by ammonia on vanadia and vanadia/titania systems [49,53,56]. NO adsorption on vanadia has also been the subject of theoretical studies. The adsorption on the oxygen sites [53], vanadium atom [48], and the hydroxyl groups [53,56] have been considered. In all the literature, the energetic effect of NO adsorption was negligible. It should be emphasized here that in these studies an NO molecule was adsorbed on the non-reduced vanadia surface, while Hadjiivanov et al. [58] and Odriozola et al. [59] concluded that NO adsorbs only on reduced divanadium pentoxide surfaces.

The main goal of the present article is to characterize and compare the properties of surface atoms in the V_2O_5 with Mo defects, modeling the MoO_3–V_2O_5 solid solution (s.s.), and the pure V_2O_5 by theoretical DFT calculations with the cluster-model approach. Furthermore, the NO adsorption on the reduced surface of V_2O_5/MoO_3–V_2O_5 s.s. has been studied. This research has been conducted to understand the influence of the molybdenum atom presence on the surface properities of MoO_3–V_2O_5 s.s., and on the NO adsorption process generally. This is the first step in a set of studies focused on direct NO decomposition on the surfaces of vanadia and molybdena–vanadia s.s.

2. Models and computational details

Divanadium pentoxide has a layer-type structure. The layers are parallel to the basal vanadia (0 0 1) surface [60] labeled (0 1 0) by Bachman and Burnes [61]. The (0 0 1) surface of V_2O_5 is composed of square – basic pyramids VO_5 (Fig. 1A). These VO_5 pyramids have common edges or corners. The pyramids that share edges form chains; parallel chains are joined by V–O–V bonds. There are three structurally different oxygen atoms coordinated to one, two, or three vanadium atoms. This leads to five different oxygen atoms on the (0 0 1) layer [O(a, b, b′, c, c′) in Fig. 1A]. The bonds between single-coordinated oxygen atoms [vanadyl oxygen, O(a) in Fig. 1A] and vanadium atoms are the shortest (1.58 Å). The length of the bonds between the other oxygen atoms and the metal are in the range of 1.78–2.01 Å. On the adjacent VO_5 pyramids, the bonds between vanadyl oxygen and the metal are perpendicular to the layer plane, located alternately up or down. It should be noted that in two edge-sharing VO_5 pyramids, the vanadium atom of one pyramid is located ca. 0.49 Å below the average surface plane and the metal atom of the other pyramid is located ca. 0.49 Å above this plane. This structural details influence the properties of the active center, which will be described later.

The interaction between adjacent vanadia (0 0 1) crystal layers is rather weak; this has been theoretically confirmed by Witko et al. [34,39]. Thus, the electronic structure of the vanadia surface can be described quite well by the model of one crystal layer. Therefore, in this paper vanadia and molybdena–vanadia solid solution surfaces are modeled by one-layer clusters embedded in a set of point charges in order to include electrostatic bulk influence. Such a one-layer model of the surface has often been used in literature for vanadia and the binary systems based on vanadia structure [12,30,31,33,47,50,51,52,54]. However, a quantitative description of the adsorption processes may require inclusion of the second layer in the cluster.

The $V_{12}O_{30}$ cluster used to model the (0 0 1) surface of pure V_2O_5 is shown in Fig. 1A. As in previous studies on V_2O_5 surface clusters, the idealized (symmetrized) geometry [31,33] is used here, with the metal–oxygen distances of 1.58 and 1.89 Å for the single- (O(a)) and the double-/triple- [O(b), O(b′), O(c), and O(c′)] coordinated oxygen, respectively. Therefore, the angles O(a)–V–O(b, b′, c, c′) are equal 104.98°.

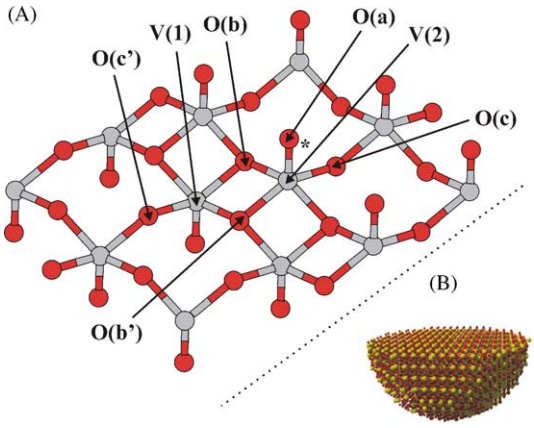

Fig. 1. (A) Structure of $V_{12}O_{30}$ cluster modeling the surface V_2O_5, the remaining clusters were obtained by a removing an oxygen atom (marked by an asterisk) and/or the substitution of the V(1) and V(2) atoms by molybdenum. (B) A general view of the hemisphere composed of point charges corresponding to all vanadium and oxygen atoms in the real V_2O_5 bulk, within a radius of 36.6 Å (10× V–V distance); the cluster used in DFT calculations is located in the middle of the surface part.

The stoichiometric $V_{12}O_{30}$ cluster is based on 12 VO_5 pyramids; six of them are entirely, and the remaining six partially included in the cluster. This cluster has been constructed to model the active-site for the NO decomposition process that is supposed to be built of two neighboring vanadium atoms, a bare surface vanadium and a vanadyl group. Thus, two edge-sharing VO_5 pyramids (active center) are located in the middle of the cluster. In order to properly represent the active-site, the remainder of the cluster is constructed in such a way that all the neighbors of the active-site atoms are included; this results in the $V_{12}O_{30}$ structure shown in Fig. 1A. It has been shown that such an approach results in a realistic charge distribution and bond-orders in the active-site region [30,33,34,39]. In most of the previous cluster studies of vanadia, molybdena, and vanadia–tungsta solid solution surfaces [12,27,28,30,31–45,47,50–52,54,55], the cluster boundaries were saturated by hydrogen atoms. Peripheral bond saturation is necessary due to the fact that the V–O bonds have a partially covalent character; thus breaking such bonds in relatively small cluster models affects the electronic properties of the active-site, and may also cause computational problems due to a high degeneracy of the cluster frontier orbitals. The cluster chosen in the present study, due to the central position of two edge-sharing VO_5 pyramids, cannot be similarly saturated by hydrogen atoms and remain stoichiometric at the same time. Therefore, we applied a different cluster-saturation scheme here. Namely, the $V_{12}O_{30}$ cluster is embedded in the hemisphere of 8904 point charges corresponding to all vanadium and oxygen atoms in the real V_2O_5 bulk, within a radius of 36.6 Å (10× V–V distance) from the center of the cluster (Fig. 1B). The vanadium and oxygen Mulliken charges obtained from the LDA calculations for the $V_{12}O_{40}H_{18}$ cluster were used. The Mulliken charges were scaled by 1/2 to avoid an overestimation of the point-charge electrostatic contribution; furthermore, the same, averaged value was used for all types of oxygen atoms, in order to guarantee a neutral model. Thus, the values of +0.65 and −0.26 were used for the V and O atoms, respectively.

The molybdena–vanadia solid solution was modeled by two $MoV_{11}O_{30}$ and $V_{11}MoO_{30}$ clusters. These models were constructed from a $V_{12}O_{30}$ cluster, in which vanadium was substituted by one molybdenum atom. In the $MoV_{11}O_{30}$ and $V_{11}MoO_{30}$ cluster, V(1) and V(2) were replaced by molybdenum (Fig. 1A), respectively. Because NO adsorbs only on reduced vanadia [58,59], three other clusters were used ($V_{12}O_{29}$, $MoV_{11}O_{29}$, $V_{11}MoO_{29}$) to model the (0 0 1) surfaces of reduced V_2O_5 and MoO_3–V_2O_5 systems. In these systems, the central vanadyl/molybdenyl oxygen was removed (Fig. 1A, the atom marked by asterisk); in such a way, the active-site for the NO adsorption has been created, built of two bare, adjacent metal atoms.

The NO adsorption on the reduced V_2O_5/MoO_3–V_2O_5 s.s. surfaces was modeled by attaching the NO molecule along the line above the V(2)/Mo(2) atom of the $V_{12}O_{29}$, $MoV_{11}O_{29}$, and $V_{11}MoO_{29}$ clusters, that is perpendicular to the surface. The cluster geometry was kept frozen and the NO distance was optimized. The present results for the large clusters follow the initial calculations for the NO adsorption on the small cluster (MoV_3O_9, similar embedding scheme) for which different NO adsorption positions and orientations were considered; these calculations indicated that the V(2)/Mo(2) site is preferred as the adsorption site (see Appendix ASupplementary data). It should be pointed out that a few factors, that have not been taken into account in the present studies, can strongly influence the calculated adsorptions energies. First of all, only one surface layer is included in the quantum-mechanically treated part of the cluster model. Thus, the effect of the second and further layers is limited to their electrostatic influence. Secondly, the surface reconstruction is not considered here. Also, the cluster embedding scheme can change both, the absolute adsorption energies, and the adsorption-site preference. However, the main goal of this study has been to investigate qualitatively the major effect of the molybdenum presence. As the model of the MoO_3–V_2O_5 solid solution is already dramatically simplified (V_2O_5 surface with Mo defects), there is no point in including more layers or surface relaxation effects.

All the calculations were performed using LCGTO-DFT program DeMon [62]. Double-zeta valence basis sets with polarization functions (DZVP) were used for all the atoms in the all-electron calculations. VWN local spin density approximation (LSDA) was used, as it is sufficient to provide a qualitative comparison of the electronic structure of the modeled systems. One should be aware, however, that calculated adsorption energies can be strongly affected by the lack of non-local effects in exchange-correlation; taking into account the simplified model of solid solution and simplified description the NO adsorption discussed in the previous paragraph, there is no need to go beyond the local approximation.

The fractional occupation numbers were used for the orbitals close to the Fermi level (corresponding to the value of 0.57 for the 'smear' parameter in the DeMon program) in order to achieve a symmetrical charge distribution at the cluster boundaries. This does not affect the charge distribution in the active-site region (center of the cluster). This idea, that changes in the 'smear' parameter would introduce negligible changes in the total energy of the system, was tested. Analysis of the electronic structure in all the clusters was conducted according to Mulliken population analysis, Mayer bond-orders, atomic (condensed) Fukui function [63–65], and molecular electrostatic potential (MEP) distribution.

3. Results and discussion

We will first discuss the electronic structure of the cluster models in terms of the Mulliken population analysis and the Mayer bond-order analysis, and then in terms of the molecular electrostatic potential distribution over the

Table 1
The Mulliken charges, Mayer bond-orders, and the atomic Fukui function (f^+) on the metal, calculated for the clusters representing the surfaces of non-reduced and reduced vanadia ($V_{12}O_{30}$, $V_{12}O_{29}$) and molybdena–vanadia solid solution ($MoV_{11}O_{30}$, $V_{11}MoO_{30}$, $MoV_{11}O_{29}$, $V_{11}MoO_{29}$)

	$V_{12}O_{30}$	$V_{12}O_{29}$	$MoV_{11}O_{30}$	$MoV_{11}O_{29}$	$V_{11}MoO_{30}$	$V_{11}MoO_{29}$
Charges						
V(1)/Mo(1)	+1.34	+1.30	+1.66	+1.61	+1.22	+1.23
V(2)/Mo(2)	+1.34	+1.29	+1.22	+1.20	+1.67	+1.34
O(a)	−0.25	–	−0.24	–	−0.24	–
O(b)	−0.74	−0.72	−0.72	−0.71	−0.73	−0.68
O(b′)	−0.74	−0.73	−0.73	−0.73	−0.72	−0.68
O(c′)	−0.56	−0.56	−0.56	−0.56	−0.56	−0.56
O(c)	−0.56	−0.51	−0.55	−0.52	−0.55	−0.49
Bond-orders						
V(1)/Mo(1)–O(b)	0.50	0.46	0.52	0.48	0.50	0.45
V(1)/Mo(1)–O(b′)	0.54	0.48	0.58	0.53	0.51	0.46
V(1)/Mo(1)–O(c′)	0.95	0.98	0.99	0.99	0.97	0.97
V(2)/Mo(2)–O(a)	2.16	–	2.16	–	1.89	–
V(2)/Mo(2)–O(b)	0.53	0.72	0.51	0.65	0.57	0.81
V(2)/Mo(2)–O(b′)	0.48	0.67	0.49	0.64	0.51	0.75
V(2)/Mo(2)–O(c)	0.94	1.21	0.97	1.20	0.98	1.19
Fukui function						
V(1)/Mo(1)	–	0.018	–	0.032	–	0.016
V(2)/Mo(2)	–	0.034	–	0.030	–	0.049

non-reduced and reduced V_2O_5 and MoO_3–V_2O_5 s.s. surfaces. Lastly, results of the calculations for the NO adsorption on the reduced surfaces will be presented.

Table 1 lists the results of the Mulliken population analysis and the Mayer bond-orders for the active center atoms in the pure/reduced vanadia and molybdena–vanadia solid solution clusters: $V_{12}O_{30}$/$V_{12}O_{29}$, $MoV_{11}O_{30}$/$MoV_{11}O_{29}$, and $V_{11}MoO_{30}$/$V_{11}MoO_{29}$. The data in Table 1 are in agreement with what could be expected, namely all metal atoms are positively charged and all oxygen atoms are negative in the clusters. As usual in these oxide-systems [33,35,36,38,40,43], the magnitude of the Mulliken charges is much smaller than the formal valences of the atoms (O^{2-}, V^{5+} in V_2O_5 and V^{4+}, Mo^{6+} in MoO_3–V_2O_5 s.s.). In agreement with previous results for V_2O_5 [33,38], the negative charge on the triply coordinated bridging oxygen atoms is the highest (−0.7) among oxygen atoms, which reflects the highest basicity of this awkward site. The values of the bond-orders are again in agreement with both the previous results [33,38,43] describing a 'double' vanadyl/molybdenyl bond (V/Mo–O(a)) and 'single' bonds between the metal and O(b, b′, c, c′). It should be pointed out that the metal–oxygen bond-orders involving the doubly coordinated O(c, c′) atoms are substantially larger (0.9) than those involving triple-coordinated O(b, b′) (0.5) atoms, which is consistent with the Mulliken population analysis-based picture indicating higher ionicity of O(b, b′).

Let us briefly discuss the effect of the molybdenum substitution in the $MoV_{11}O_{30}$ and $V_{11}MoO_{30}$ clusters, in which V(1) and V(2) were substituted by Mo in $MoV_{11}O_{30}V_{11}MoO_{30}$, respectively. The results of Table 1 demonstrate that in these systems, the adjacent vanadium atom becomes smaller (change in the charge from 1.34 to 1.22), while the positive charge located on molybdenum is somewhat larger (1.66, 1.67) and close to the Mo charge in MoO_3 (1.67) [32,40]. It should be noted that an increase in the molybdenum charge appears solely at the expense of the vanadium charge: the populations on all the oxygen sites practically do not change. This is in qualitative agreement with earlier experimental results [1] demonstrating vanadium reduction due to the substitution of molybdenum for vanadium. Similarly, there is only a minor effect on the bond-order values. The changes due to molybdenum substitution do not exceed 0.04 for the bonds involving O(b, b′, c, c′). The only pronounced difference may be observed for the Mo–O(a) molybdenyl bond, which is much weaker (1.89) than the corresponding vanadyl bond (2.16). This fact reflects an increased ionicity of the molybdenyl bond and is consistent with the results of the population analysis. Negligible changes in the results obtained for oxygen atoms with a change of the metal seem to indicate that the properties of oxygens atoms are mainly determined by cluster geometry.

Let us now discuss the cluster models of the reduced surface of vanadia and molybdena–vanadia s.s. The result of Table 1 demonstrate that the effect of surface reduction depends on the molybdenum position relative to removed oxygen. Namely, in the $V_{12}O_{29}$, $MoV_{11}O_{29}$ clusters in which the vanadyl oxygen atom was removed, both metal atoms are reduced. In the pure-vanadium cluster, the reduction of both vanadium atoms is quite similar (change in the charge from 1.34 to 1.30–1.29), whereas in the $MoV_{11}O_{29}$ cluster the change in the charge is slightly larger for Mo(1) (from 1.66 to 1.61) than for the V(2) atom (from 1.22 to 1.20) from which the oxygen was removed. Metal atoms can be

observed to behave differently in the $V_{11}MoO_{29}$ cluster, which has one fewer oxygen atom. Namely, the Mo(2) atom is substantially reduced (from 1.67 to 1.34), while the V(1) atom hardly changes its charge (from 1.22 to 1.23).

The results of Table 1 also show that, similarly to the non-reduced clusters, a reduction of the adjacent metal atom is accompanied by practically no change in the oxygen populations. Here, however, the effect is slightly stronger due to the fact that in the reduced surfaces the molybdenum atom is coordinatively unsaturated (coordination number 4).

Let us now consider the molecular electrostatic potential (MEP) distribution for all the clusters studied in the present work. The MEP values describe the electrostatic interaction of the cluster with an external (positive) point charge at the position ***r***. This quantity can, therefore, be used to identify regions in which external particles can be stabilized due to electrostatic interaction with a molecular system, and as such it is widely used in diagnosing chemical reactivity. The molecular electrostatic potential distribution was previously studied for both, vanadium and molybdenum oxide surface-clusters [12,32,33,42,47]. For all the clusters in the present work, the MEP values were determined for two cuts through the active-site region (perpendicular to the surface), as well as for a plane parallel to the surface, located 3.23 Å above the V(2)/Mo(2) atom; this distance corresponds to the minimum of MEP above the O(a) atom in the $V_{12}O_{30}$ cluster. Since both 'perpendicular' cuts lead to similar conclusions, we present the most important MEP maps for one cut only. The remaining plots as well as the set of contour maps for the second cut is included in Supplementary data.

In the case of the 'perpendicular' cut discussed here, two metal atoms of the active-site [V(1)/Mo(1) and V(2)/Mo(2)] and the O(a) oxygen atom are located in the plot plane. In all the contour maps, solid lines correspond to positive MEP values, while the dashed lines describe the negative MEP regions. The contours are plotted with an increment of ±0.001 a.u.; for clarity the contours representing the values grater than +0.02 a.u. were omitted.

In Fig. 2, the contour map of MEP, calculated for the $V_{12}O_{30}$ and $V_{12}O_{29}$ clusters for the 'perpendicular' cut through the two active-site metal centers are shown. The first plot (Fig. 2A) describes a pure V_2O_5 surface, while the second (Fig. 2B) describes a reduced surface. The MEP of Fig. 2A exhibits features similar to those published previously for hydrogen-saturated V_2O_5-clusters [12,33,42,47]: a broad region of negative MEP extends over the surface, with a minimum located in the vicinity of vanadyl oxygen, O(a). It is not surprising, that the MEP minimum disappears as an effect of surface reduction, i.e. vanadyl oxygen removal. The positive MEP area above the bare-metal-centers extends up to a distance of 2–3 Å; for larger distances MEP becomes negative. It should be noted that due to surface geometry, the MEP distribution in the vicinity of the two bare-metal-atoms is asymmetric: the positive MEP region extends further above the metal atom in position (2). It should also be pointed out that for the reduced

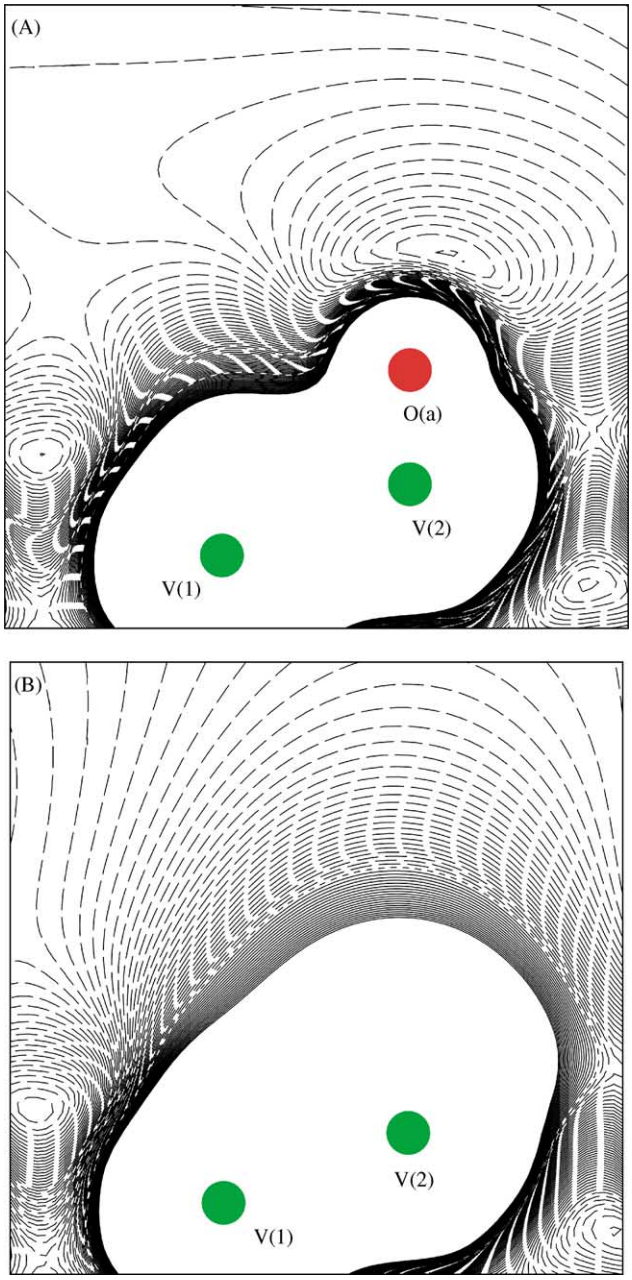

Fig. 2. Contour plots of the molecular electrostatic potential (MEP) in the plane containing V(1), V(2), and O(a) atoms for the $V_{12}O_{30}$ (A) and $V_{12}O_{29}$ (B) clusters. The solid lines correspond to the positive MEP values, while the dashed lines represent the negative MEP values. The contours are plotted with an increment of ±0.001 a.u. The contours corresponding to the values greater than +0.02 a.u. were omitted for clarity.

clusters the positive values located in the vicinity of the metal center extend slightly further above the center, compared to the clusters without an oxygen vacancy. Thus, at similar distances above the surface the MEP values are slightly less negative for the reduced cluster. This is in agreement with a chemist's basic intuition.

However, the effect of substituting molybdenum for vanadium could not be predicted without the proper calculations. Therefore, similar contour maps have been

prepared for the two MoO_3–V_2O_5 s.s. clusters, $MoV_{11}O_{30}$ and $V_{11}MoO_{30}$, and their reduced derivatives, $MoV_{11}O_{29}$, and $V_{11}MoO_{29}$. These maps are qualitatively indistinguishable from those of Fig. 2. Therefore, in order to elucidate the molybdenum substitution effect, it seems to be more convenient to plot the differences between the maps for the V_2O_5-clusters and the corresponding MoO_3–V_2O_5 s.s. models. Such differential plots for the reduced surfaces are presented in Fig. 3. Fig. 3A shows that substitution of V(1) by Mo(1) results in an increase of the MEP values above the Mo(1) center. This is accompanied by practically no change

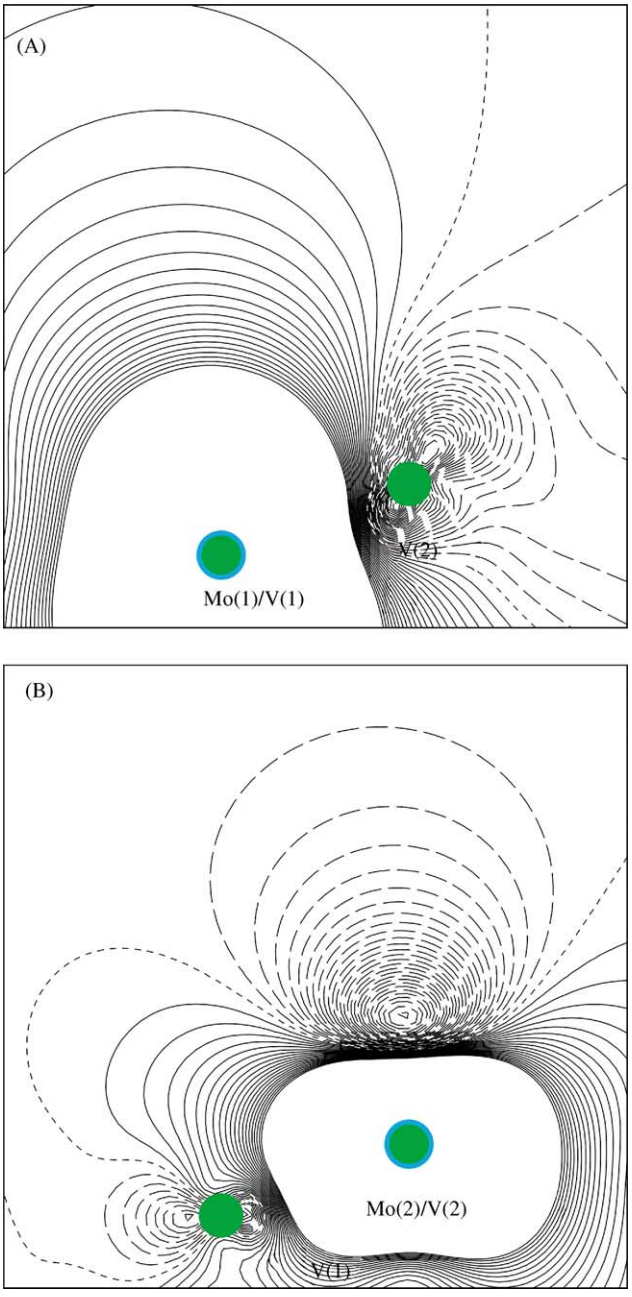

Fig. 3. Contour plots of the difference in the molecular electrostatic potential between the $MoV_{11}O_{29}$ and $V_{12}O_{29}$ clusters (A), $V_{11}MoO_{29}$ and $V_{12}O_{29}$ clusters (B). The contour details are as in Fig. 2.

above the other active-site metal [V(2)], substituting molybdenum for the adjacent vanadium leads to the more pronounced changes shown in Fig. 3B. It is surprising that in this case the molybdenum-substitution results in a decrease of MEP above this center, not an increase. This may be attributed to the 'size' of the metal, and the fact that bare-Mo electron density extends further than that of V.

Let us now consider the MEP contour maps for the reduced clusters plotted in the plane 'parallel' to the surface (3.23 Å above the V(2)/Mo(2) atom) shown in Fig. 4. It can be observed that as a result of the surface reduction by O(a) removal, the MEP above V(2)/Mo(2) atoms is positive, while at this distance from the surface, it is negative elsewhere. This clearly indicates that the V(2)/Mo(2) center can act as a site for NO adsorption, as the MEP of the NO molecule exhibits a broad negative region in the vicinity of the nitrogen atom. Therefore, the adsorbate should be stabilized over the metal atom in position (2).

It should be noted that the MEP plots of Fig. 4 also show the aforementioned effect of the Mo substitution, which is opposite for the two positions. Substituting Mo for the V(1) atom increases the positive MEP, while the substitution of V(2) leads to a decrease in MEP. Such a decrease above Mo(2) of the reduced MoO_3–V_2O_5 s.s. should result in a destabilization of a nucleophilic agent approaching this site, compared to V(2) of both the $V_{12}O_{29}$ and $MoV_{11}O_{29}$ clusters. However, MEP only describes the electrostatic component of the interaction. Therefore, in order to account for the complementary frontier-orbital component, we calculated the Fukui function (FF) for electron addition (f^+) [63,64] of the metal atom in reduced clusters. The calculated atomic FF values are included in the last part of Table 1. The Fukui function has been widely used as a single-reactant chemical reactivity descriptor [65]; maximum positive values of the FF index indicate the preferred site for chemical bond formation. The data in Table 1 clearly show that the FF value for the Mo(2) atom in the $V_{11}MoO_{29}$ cluster is substantially higher (0.049) than for other cases (0.018–0.034). Thus, the FF indicates that Mo(2) in the preferred NO adsorption site. This is contrary to the MEP-based prediction that electrostatic and frontier-orbital components behave in opposite ways. Therefore, in this case, it is difficult to predict the consequences of the V substitution by Mo for the NO adsorption on the basis of the calculations for the clusters only (without considering the whole reactive system).

Let us now consider the results of the DFT calculations for NO adsorption on the metal centers of the reduced clusters. Table 2 lists the adsorption energy, the metal–nitrogen and the N–O inter-atomic distances as well as the corresponding Mayer bond-orders for the NO complexes with the $V_{12}O_{29}$, $MoV_{11}O_{29}$, and $V_{11}MoO_{29}$ clusters modeling the reduced surfaces. In all cases, the adsorption on the reduced surfaces is exothermic, with energies of ca. 80 kcal/mol. The energetic stabilization is the largest for the $V_{11}MoO_{29}$ (−82 kcal/mol). At this point, we would like to

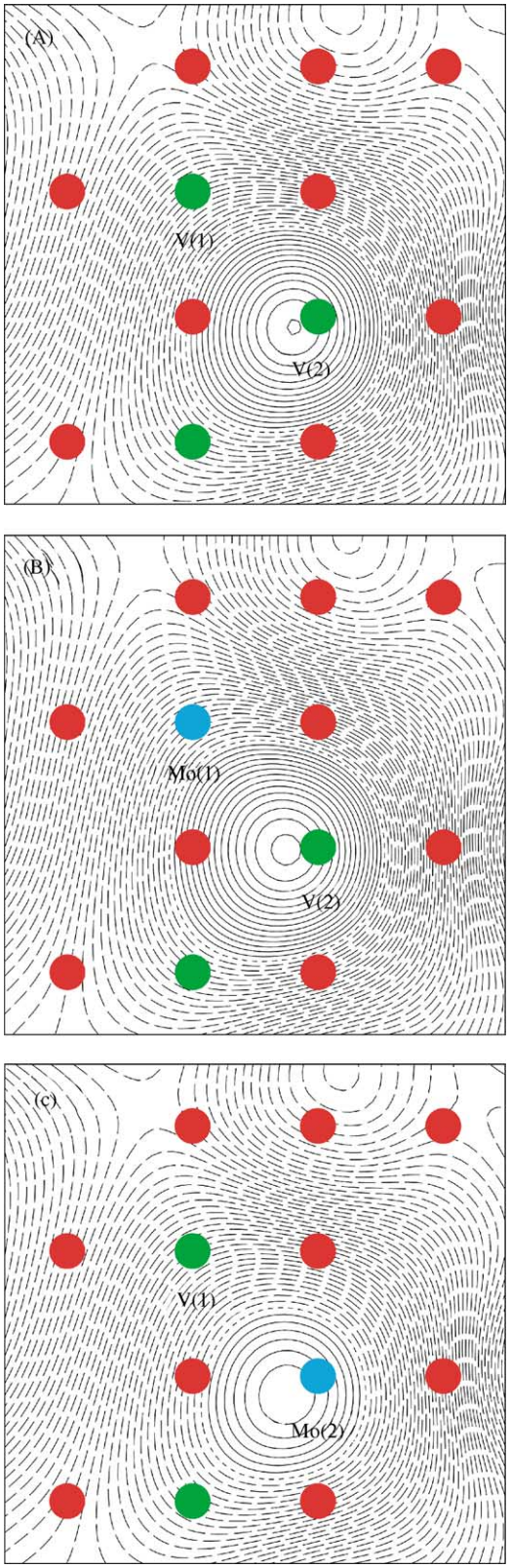

Fig. 4. Contour plots of the molecular electrostatic potential in the plane parallel to the surface (3.23Å above the V(2)/Mo(2) atom) for: the $V_{12}O_{29}$ cluster (A), the $MoV_{11}O_{29}$ cluster (B) and the $V_{11}MoO_{29}$ cluster (C). The contour details are as in Fig. 2.

Table 2
The adsorption energy (E_{ads}), Me–N, and N–O inter-atomic distances (R_{Me-N} and R_{NO}) and the corresponding Mayer bond-orders (B_{MeN} and B_{NO}) for the complexes involving NO adsorbed on the V(2)/Mo(2) atom of the $V_{12}O_{29}$, $V_{11}MoO_{29}$, and $MoV_{11}O_{29}$ clusters

	$V_{12}O_{29}$	$MoV_{11}O_{29}$	$V_{11}MoO_{29}$
E_{ads} (kcal/mol)	−79.56	−78.73	−82.02
R_{Me-N} (Å)	1.720	1.720	1.800
B_{MeN}	1.15	1.23	1.21
R_{NO} (Å)[a]	1.177	1.177	1.177
B_{NO}[b]	1.76	1.72	1.69

[a] 1.167 Å for isolated NO molecule.
[b] 2.24 for isolated NO molecule.

emphasize again that many effects not taken into account in the present study can affect calculated adsorption energies, such as simplified description of the system (one-layer active center), lack of surface reconstruction, simplified computational methodology (LDA). Thus, the calculated absolute adsorption energies are likely to be highly overestimated. The major conclusion from the calculations presented here is that the adsorption energies for the three considered cases are similar, differing only by ca. 12 kJ/mol, i.e. ca. 3 kcal/mol. Thus, there is no pronounced effect of the Mo presence.

The data in Table 2 demonstrate that in all the cases studied, a strong chemical bond between the adsorbate and the surface metal is formed: the metal–nitrogen distance in an equilibrium geometry is 1.7–1.8 Å, and the corresponding bond-order value varies in the range of 1.15–1.23. As a result, the NO bond becomes weaker (bond-order lowering from 2.24 in NO to 1.76, 1.72 and 1.69 in $V_{12}O_{29}$, $MoV_{11}O_{29}$, $V_{11}MoO_{29}$ clusters, respectively). These effects are also reflected by the NO bond length: an elongation from 1.166 Å (in the isolated NO molecule) to 1.177 Å (after adsorption on each cluster). Thus, the present results demonstrate that surface reduction leads to a stable NO adsorption, but the effect of substituting V by Mo is almost negligible.

4. Conclusions

The clusters modeling the surface of reduced and non-reduced vanadia and molybdena–vanadia solid solution were constructed and their electronic structure was investigated by DFT calculations. Surface reduction was modeled by removing vanadyl/molybdenyl oxygen atoms. For all clusters, the electronic structures were analyzed using Mulliken population analysis, Mayer bond-orders and molecular electrostatic potential plots. The properties of the surface atoms were analyzed with a special emphasis on the effect of the molybdenum substitution and the surface reduction. NO adsorption on the reduced surface of V_2O_5/MoO_3–V_2O_5 s.s. was also studied.

The results indicate that the replacement of V by Mo causes a reduction in the adjacent vanadium atom. Changes in metal populations (compared to V_2O_5 model) appear at

the expense of the vanadium charge and the populations on all the oxygen sites practically do not change. The plots of molecular electrostatic potential show a broad region of negative MEP extending over the surface, with a minimum located in the vicinity of the terminal oxygen O(a).

The effect of surface reduction is most visible for the unsaturated metal with a decreasing charge. However, as a result of oxygen removal, the MEP above the created bare-metal-site exhibits more positive values. At the distance corresponding to the MEP minimum observed in the non-reduced clusters, here the positive MEP 'islands' clearly point to the prospective NO adsorption sites. Furthermore, in the reduced clusters, the effect of the Mo substitution is different for the two analyzed positions: substituting Mo(1) for V(1) increases the MEP values above the Mo(1) center. However, substitution in position (2) decreases MEP values in Mo(2) surroundings. On the other hand, atomic Fukui function values indicate that the Mo(2) center in the reduced cluster is the preferred site for a nucleophilic attack.

NO adsorption results indicate that the surface reduction leads to a stable NO adsorption. The calculated stabilization of ca. 80 kcal/mol is likely to be overestimated due to a simplified cluster representation, lack of surface reconstruction, the cluster embedding scheme, and the use of local exchange-correlation. The main qualitative conclusion from the present studies is that the effect of the molybdenum presence is not very distinct. Further studies on the elementary reactions in direct NO decomposition are in progress.

Acknowledgement

This paper was partially supported by a grant from KBN (Grant No. 4T09A 12725).

Appendix A. Supplementary data

Supplementary data associated with this article can be found, in the online version, at 10.1016/j.cattod.2005.01.015.

References

[1] A. Bielanski, M. Najbar, Appl. Catal. A 157 (1997) 223.
[2] H. Bosh, P. Jansen, Catal. Today 2 (1988) 369.
[3] C. Cristiani, P. Forzatti, J. Catal. 116 (1989) 586.
[4] G.T. Went, L.-J. Leu, R.R. Rosin, A.T. Bell, J. Catal. 134 (1992) 492.
[5] U.S. Ozkan, Y. Cai, M. Kumthekar, L. Zhang, J. Catal. 142 (1993) 182.
[6] L. Lietti, P. Forzatti, J. Catal. 147 (1994) 241.
[7] N.Y. Topsoe, H. Topsoe, J.A. Dumesic, J. Catal. 151 (1995) 226.
[8] P. Forzatti, L. Lietti, HCR Compr. Rev. 3 (1996) 33.
[9] G. Busca, L. Lietti, G. Ramis, F. Berti, Appl. Catal. B 18 (1998) 1.
[10] M. Amiridis, R. Duevel, I. Wachs, Appl. Catal. B 20 (1999) 111.
[11] L. Lietti, I. Nova, P. Forzatti, Top. Catal. 11–12 (2000) 111.
[12] M. Najbar, J. Banaś, J. Korchowiec, A. Białas, Catal. Today 73 (2002) 249.
[13] P. Kornelak, J. Banaś, A. Białas, M. Najbar, in: Proceedings of the Jumelage-Matériaux Carbonés et Catalytiques pour L'Environnement, Zakopane, 3–8 October, 2002, p. 225.
[14] J. Banaś, J. Korchowiec, A. Wesełucha-Birczyńska, M. Najbar, in: Proceedings of the Jumelage-Matériaux Carbonés et Catalytiques pour L'Environnement, Zakopane, 25–30 September, 2003, p. 327.
[15] P. Kornelak, F. Mizukami, A. Wesełucha-Birczyńska, E. Bielańska, L. Lityńska-Dobrzyńska, G. Djega-Mariadassou, M. Najbar, in: Proceedings of the Jumelage-Matériaux Carbonés et Catalytiques pour L'Environnement, Zakopane, 25–30 September, 2003, p. 321.
[16] P. Kornelak, D. Su., J. Banaś, C. Thomas, E. Bielańska, J. Camra, A. Wesełucha-Birczyńska, M. Najbar, in preparation.
[17] E. Brocławik, D.R. Salahub, J. Mol. Catal. 82 (1993) 117.
[18] E. Brocławik, Catal. Today 23 (1995) 379.
[19] E. Brocławik, in: J.M. Seminario, P. Politzer (Eds.), Modern Density Functional Theory: A Tool for Chemistry Theoretical and Computational Chemistry, vol. 2, Elsevier Science B.V., 1995, p. 349.
[20] E. Brocławik, T. Borowski, Chem. Phys. Lett. 339 (2001) 433.
[21] E. Brocławik, D.R. Salahub, Int. J. Quantum Chem. 52 (1994) 1017.
[22] J. Oliveira, W.B. De Almeida, H.A. Duarte, Chem. Phys. Lett. 372 (2003) 650.
[23] E. Brocławik, W. Piskorz, K. Adamska, J. Chem. Phys. 110 (1999) 11685.
[24] S. Vyboishchikov, J. Sauer, J. Phys. Chem. A 105 (2001) 8588.
[25] M. Calatayud, B. Mguig, C. Minot, Surf. Sci. 526 (2003) 297.
[26] A. Chakrabarti, K. Hermann, R. Druzinic, M. Witko, F. Wagner, M. Petersen, Phys. Rev. B 59 (1999) 10583.
[27] E. Brocławik, M. Łabanowska, Bull. Pol. Acad. Sci. 48 (2000) 303.
[28] E. Brocławik, M. Łabanowska, A. Jurkiewicz, Bull. Pol. Acad. Sci. 50 (2002) 359.
[29] J. Haber, M. Witko, Catal. Today 23 (1995) 311.
[30] M. Witko, Catal. Today 32 (1996) 89.
[31] K. Hermann, A. Michalak, M. Witko, Catal. Today 32 (1996) 321.
[32] A. Michalak, K. Hermann, M. Witko, Surf. Sci. 366 (1996) 323.
[33] A. Michalak, M. Witko, K. Hermann, Surf. Sci. 375 (1997) 385.
[34] M. Witko, R. Tokarz, J. Haber, Appl. Catal. A 157 (1997) 23.
[35] M. Witko, R. Tokarz, K. Hermann, Pol. J. Chem. 72 (1998) 1565.
[36] M. Witko, R. Tokarz, K. Hermann, Collect. Czech. Chem. Commun. 63 (1998) 1355.
[37] K. Hermann, A. Chakrabarti, R. Druzinic, M. Witko, Phys. Stat. Sol. A 173 (1999) 195.
[38] K. Hermann, M. Witko, R. Druzinic, Faraday Discuss. 114 (1999) 53.
[39] M. Witko, K. Hermann, R. Tokarz, Catal. Today 50 (1999) 553.
[40] K. Hermann, M. Witko, A. Michalak, Catal. Today 50 (1999) 567.
[41] K. Hermann, M. Witko, R. Druzinic, R. Tokarz, Top. Catal. 11–12 (2000) 67.
[42] M. Witko, K. Hermann, R. Tokarz, R. Druzinic, A. Chakrabarti, in: N. Russo, D. Salahub (Eds.), Metal Ligand Interactions in Chemistry, Physics and Biology, NATO Science Series C, vol. 546, Kluwer Academic Publishers, 2000, p. 417.
[43] K. Hermann, M. Witko, in: D.P. Woodruff (Ed.), The Chemical Physics of Surfaces, Oxide Surfaces, vol. 9, Elsevier, New York, 2001, p. 136(Chapter 4).
[44] K. Hermann, M. Witko, R. Druzinic, R. Tokarz, Appl. Phys. A 72 (2001) 429.
[45] R. Tokarz-Sobieraj, K. Hermann, M. Witko, A. Blume, G. Mestl, R. Schlögl, Surf. Sci. 489 (2001) 107.
[46] J. Haber, M. Witko, J. Catal. 216 (2003) 416.
[47] J. Korchowiec, J. Banaś, M. Najbar, Chem. Phys. Lett. 371 (2003) 253.
[48] T. Homann, T. Bredow, K. Jug, Surf. Sci. 515 (2002) 205.
[49] F. Gilardoni, J. Weber, A. Baiker, J. Phys. Chem. A 101 (1997) 6069.
[50] A. Góra, E. Brocławik, M. Najbar, Comput. Chem. 24 (2000) 405.
[51] A. Góra, E. Brocławik, Pol. J. Environ. Stud. 9 (2000) 31.
[52] M. Najbar, E. Brocławik, A. Góra, J. Camra, A. Białas, A. Wesełucha-Birczyńska, Chem. Phys. Lett. 325 (2000) 330.

[53] X. Yin, H. Han, A. Miyamoto, Phys. Chem. Chem. Phys. 2 (2000) 4243.
[54] E. Brocławik, A. Góra, M. Najbar, J. Mol. Catal. A 166 (2001) 31.
[55] N. Topsøe, M. Anstrom, J.A. Dumesic, Catal. Lett. 76 (2001) 11.
[56] M. Anstrom, N. Topsøe, J.A. Dumesic, J. Catal. 213 (2003) 115.
[57] A. Klisińska, A. Haras, K. Samson, M. Witko, B. Grzybowska, J. Mol. Catal. A 210 (2004) 87.
[58] K. Hadjiivanov, P. Concepción, H. Knözinger, Top. Catal. 11–12 (2000) 123.
[59] J.A. Odriozola, H. Heinemann, G.A. Somorjai, J.F. Garcia de la Banda, P. Pereira, J. Catal. 119 (1989) 71.
[60] JCPDS, Card 9–387, Nat. Bur. Stand. Circ. 539 (8) (1958) 66.
[61] H.G. Bachman, W.H. Burnes, Z. Kristellogr. 115 (1961) 215.
[62] A. St. Amant, D.R. Salahub, Chem. Phys. Lett. 169 (1990) 387; A. St. Amant, Université de Montréal, Ph.D. thesis, Montréal, 1991.
[63] R.G. Parr, W. Yang, J. Am. Chem. Soc. 106 (1984) 4049.
[64] W. Yang, W. Mortier, J. Am. Chem. Soc. 108 (1986) 5708.
[65] P. Geerlings, F. DeProft, W. Langenaeker, Chem. Rev. 103 (2003) 1793, and references therein.